This is a preprint, the final version is subject to change, of the American Mineralogist (MSA)
Cite as Authors (Year) Title. American Mineralogist, in press.
DOI: https://doi.org/10.2138/am-2020-7192

Revision 1

Negevite, the pyrite-type NiP_2, a new terrestrial phosphide

Sergey N. Britvin[1,2]*, Michail N. Murashko[1], Ye. Vapnik[3], Yury S. Polekhovsky[1†], Sergey V. Krivovichev[2,1], Oleg S. Vereshchagin[1], Vladimir V. Shilovskikh[1,4], and Maria G. Krzhizhanovskaya[1]

[1]St. Petersburg State University, Universitetskaya Nab. 7/9, 199034 St. Petersburg, Russia

[2]Kola Science Center, Russian Academy of Sciences, Fersman Str. 14, 184209 Apatity, Russia

[3]Department of Geological and Environmental Sciences, Ben-Gurion University of the Negev, P.O.B. 653, Beer-Sheva 84105, Israel

[4]Institute of Mineralogy, Urals Branch of Russian Academy of Science, Miass 456317, Russia

†Deceased: September 29, 2018.

Abstract

Negevite, ideally NiP_2, is a new phosphide mineral from pyrometamorphic complex of the Hatrurim Formation (the Mottled Zone), Southern Levant. It is found in phosphide assemblages of the Hatrurim Basin, south Negev Desert, Israel, and Daba-Siwaqa complex, Jordan. The mineral occurs as tiny isometric grains reaching 15μm in size, and forms intimate intergrowths with other phosphides related to the Fe-Ni-P system. In reflected light, negevite is white with yellowish tint. Isotropic. Reflectance values for COM recommended wavelengths [R (%), λ (nm)] are as follows: 54.6 (470), 55.0 (546), 55.3 (589), 55.6 (650). Chemical composition of the holotype specimen (electron microprobe, wt%): Ni 42.57, Co 3.40, Fe 2.87, P 42.93, S 8.33, total 100.10, corresponding to the empirical formula $(Ni_{0.88}Co_{0.07}Fe_{0.06})_{\Sigma 1.01}(P_{1.68}S_{0.31})_{\Sigma 1.99}$. The crystal structure of negevite was solved and refined to R_1 = 1.73% based on 52 independent observed [$I > 2\sigma(I)$]

reflections. The mineral is cubic, space group $Pa\bar{3}$, a 5.4816(5) Å, V 164.71(3) Å^3, and $Z = 4$. D_x = 4.881(1) g/cm^3 calculated on the basis of empirical formula. Negevite is a first natural phosphide belonging to the pyrite structure type. It is a chemical and structural analog of vaesite, NiS_2, krutovite, $NiAs_2$, and penroseite, $NiSe_2$. The well explored catalytic and photocatalytic properties of a synthetic counterpart of negevite could provide new insights into the possible role of higher phosphides as a source of low-valent phosphorus in prebiotic phosphorylation processes.

Keywords: NiP_2, negevite, nickel phosphide, Fe-Ni-P system, pyrite, crystal structure, pyrometamorphism, prebiotic phosphorylation, meteorite

Introduction

Since the discovery of first phosphide mineral, schreibersite $(Fe,Ni)_3P$ (Berzelius 1832), natural iron-nickel phosphides were recognized as mandatory accessory constituents of different meteorite groups (Buchwald 1975; Papike 1998). This mineral family is suggested to play an important role in the highly reduced assemblages of deep planetary interiors (Scott et al. 2007; Dera et al. 2008; Gu et al. 2011, 2012, 2014). Meanwhile, occurrences of terrestrial phosphides of non-anthropogenic origin are quite rare and confined to a few localities worldwide (e.g., Britvin et al. 2015); the most notable one is schreibersite in native iron from basalts of Disko Island, Greenland (Pauly 1969). The practical absence of phosphides in the present-day lithosphere can not be accounted just for highly reducing conditions required for their formation. A possible explanation might imply oxidative decomposition of phosphides at the early stages of Earth evolution, leading to a release of low-valent phosphorus required for initiation of prebiotic phosphorylation processes (Pasek et al. 2017; Kitadai and Maruyama 2018; Gibard et al. 2019). The recent discovery of rich phosphide assemblages preserved in geologically juvenile pyrometamorphic complex of the Mottled Zone (Hatrurim Formation) supports this point of view (Britvin et al. 2015).

Of twelve phosphide minerals related to the Fe-Ni-P system, nine are currently reported from the Hatrurim Formation (Table 1). We herein present the results of a study of a new mineral negevite, NiP_2 - the first natural phosphide which crystallizes in a pyrite structure type. Negevite is named for its type locality in the Negev Desert, Israel; both the mineral and the name have been approved by the Commission on New Minerals, Nomenclature and Classification of International Mineralogical Association (IMA 2013-104). The holotype specimen of negevite is deposited in the collections of the Mineralogical Museum of the Department of Mineralogy, St. Petersburg State University, St. Petersburg, Russia, catalogue number 19604.

Occurrence and general appearance

The Mottled Zone is the world's widest area of sedimentary rocks affected by combustion metamorphism – the suite of processes leading to high-temperature annealing and melting of surficial sediments (Sokol et al. 2005). Outcrops of the Mottled Zone are scattered across the territory of 150 × 200 km^2 in Southern Levant in the surroundings of the Dead Sea. The detailed description of geological setting along with the hypotheses explaining origin of the Mottled Zone are given in previous works (Gross 1977; Burg et al. 1991; Vapnik et al. 2007; Geller et al. 2012; Novikov et al. 2013). Metamorphic processes were followed by pronounced hydrothermal alteration and weathering stage (Gross 1977; Kolodny et al. 2014), that resulted in emergence of unique mineral assemblages, combining ultrahigh-temperature minerals (Weber and Bischoff 1994; Murashko et al. 2010; Sharygin et al. 2013; Galuskina et al. 2014; Khoury et al. 2016) and secondary phases corresponding to Earth's extreme oxidative and/or alkaline environment (Hauff et al. 1983; Sokol et al. 2011; Galuskin et al. 2013, 2014).

Negevite was discovered in phosphide assemblages found along the upper stream of the Halamish Wadi, Hatrurim Basin, Southern Negev desert, Israel (Britvin et al. 2015). The mineral forms irregular minute grains up to 15μm in size intimately intergrown with murashkoite,

zuktamrurite, transjordanite or halamishite (Fig. 1). Phosphide assemblages often occur together with magnetite, pyrrhotite and andradite in diopside microbreccia which is severely altered by hydrothermal and weathering processes (Fig. 1). Secondary minerals are comprised by calcite and unidentified X-ray amorphous Ca-Fe hydrous silicates and phosphates. The Hatrurim Basin is a type locality for negevite. Later on, the mineral was identified in one sample of weathered pyrometamorphic paralavas of the Daba-Siwaqa complex (Um Al-Rasas Sub-District, 80 km SSE of Amman, Jordan, 31° 21' 52" N, 36° 10' 55" E) where it forms micrometer-sized aggregates of irregularly fractured grains often intergrown with transjordanite and zuktamrurite (Fig. 2).

Physical properties and chemical composition

In reflected light, negevite has a white color with bluish tint (Fig. 1A). It is optically isotropic and has no internal reflections. Reflectance values (Table S1) were measured in air by means of a MSF-21 spectrophotometer (LOMO, St. Petersburg, Russia) using monochromator slit of 0.4mm and beam diameter of 0.1mm, against WTiC standard. The mineral has no observable cleavage. Due to small size of the grains available, microindentation hardness could not be measured. The calculated density of the holotype specimen calculated for an empirical formula is 4.881(1) g/cm^3. Negevite is insoluble in cool 10% HCl. Chemical composition of negevite and associated phosphides was studied in carbon-coated polished thick sections by means of a Hitachi S-3400N scanning electron microscope equipped with (1) an Oxford Instruments AzTec Energy X-Max 20 energy dispersive (EDX) spectrometer and (2) an INCA WAVE 500 wavelength-dispersive (WDX) spectrometer. Preliminary screening of chemical composition and elemental mapping (Fig. 1C, 1D) was carried out in EDX mode whereas quantitative data (Table 1) were obtained with WDX spectrometer using the following analytical standards: GaP (P*K*α), pyrite (Fe*K*α, S*K*α), PbSe (Se*L*α), metallic Co (Co*K*α), Ni (Ni*K*α), Mo (Mo*L*α), Ag (Ag*L*α). The measurement conditions were: 20kV accelerating voltage, 15nA beam current, peak counting time, 20s peak counting time; 10s background counting

time. Chemical composition of the holotype negevite (Table 2) corresponds to the empirical formula $(Ni_{0.88}Co_{0.07}Fe_{0.06})_{\Sigma 1.01}(P_{1.68}S_{0.31})_{\Sigma 1.99}$ leading to the ideal formula NiP_2.

X-ray single crystal study

In order to establish and refine the crystal structure of negevite, a ~10μm single-crystal grain of the mineral was extracted from the polished section, mounted onto the glass fiber and subjected to a conventional X-ray single-crystal data collection by means of a Bruker APEX Kappa DUO CCD diffractometer. Data processing and integration routines were performed using a Bruker AXS instrument built-up software (Bruker 2003). The crystal structure of negevite was solved by direct methods and refined assuming NiP_2 formula, by means of a *SHELX*-2018 software (Sheldrick 2015) incorporated into Olex2 program environment (Dolomanov et al. 2009). The essential parameters of data collection and structure refinement are summarized in Table S2; the complete structural information can be retrieved from the CIF file in the Supplementary Data (see also CSD entry 1936174). The insufficient amount of substance had precluded obtaining experimental X-ray powder diffraction data for the mineral. Therefore, powder diffraction pattern of negevite was calculated for Cu*K*α1 radiation on the basis of refined atomic coordinates and unit cell metrics, using ATOMS v.5.0 software (Dowty 2006) (Table S3).

Discussion

Negevite is the first natural phosphide related to a pyrite structure type (Fig. 3). From the crystal-chemical point of view, the mineral can be regarded as phosphide analog of either vaesite, NiS_2, krutaite, $NiAs_2$, and penroseite, $NiSe_2$ (Table 3). Though the ideal formula of negevite is NiP_2, its real composition shows substantial (up to 0.48 atoms per MX_2 formula) contents of sulfur (Table 2), suggesting the occurrence of at least partial isomorphism along the join NiP_2 – NiS_2. Substitution of

125 P for S correlates with an increase of the unit cell parameter of negevite as compared to pure NiP_2
126 (Table 3).

127 Contrary to the synthetic marcasite-type FeP_2 and its natural analog, zuktamrurite (Table 1),
128 NiP_2 can exist in two polymorphic modifications, both of which are stable under ambient conditions:
129 (1) cubic, pyrite-type one (Donohue et al. 1968) and (2) monoclinic polymorph (space group *C*2/*c*)
130 which has no sulfide or phosphide structural analogs (Larsson 1965; Orishchin et al. 2000).
131 Synthetic pyrite-type NiP_2 was first synthesized under high-pressure-temperature environment and
132 thus was considered to be metastable, high-pressure polymorph of NiP_2 (Donohue et al. 1968).
133 However, further studies revealed that this modification can be obtained using different methods at
134 atmospheric pressure: via solid-state synthesis (Barry and Gillan 2009) and even by "soft chemistry"
135 solvothermal techniques (Barry and Gillan 2008). Because NiP_2 was found to be promising material
136 in modern electrochemical and catalytic applications (Gillot et al. 2005; Jiang et al. 2014), its
137 chemical and physical characteristics were studied in detail. In particular, it was determined that
138 pyrite-type NiP_2 is a low-temperature modification stable below 600°C (Owens-Baird et al. 2019).
139 Moreover, it was shown that transformation of cubic NiP_2 into the monoclinic modification is
140 irreversible, implying that the presence of cubic NiP_2 in a given assemblage evidences that the
141 temperature has never passed the level of cubic-to-monoclinic transition (Owens-Baird et al. 2019).
142 These results could be helpful in understanding the formation conditions of natural phosphide
143 assemblages of the Mottled Zone (Britvin et al. 2015). However, the presence of sulfur in the
144 composition of natural negevite (Table 2) might stabilize its pyrite-type structure towards higher
145 transition temperature.

146 An interesting feature of negevite from the Daba-Siwaqa complex in Jordan is its relative
147 enrichment in Ag (Table 2). It becomes even more attractive taking into account the absence of Ag
148 in closely associated zuktamrurite, FeP_2, and transjordanite, Ni_2P (Fig. 2, Table 2). Ag is an element
149 which is structurally incompatible with Ni. Synthetic phosphide AgP_2 is known though it is not

isostructural with negevite (Möller and Jeitschko 1982). Recent investigation of Ag-doped synthetic pyrite demonstrated that it may contain up to 0.4 wt% (3820ppm) Ag incorporated via mechanism of lattice-scale structural defects (Li and Ghahreman 2018). Therefore, one can assume that minor (0.01 atoms per formula unit) incorporation of Ag into negevite is also permissible.

Implications

Discovery of negevite, naturally occurring NiP_2 might have promising implications considering the general role of phosphides as a source of phosphorus required for phosphorylation processes. It was shown that gentle aquatic oxidation of schreibersite, $(Fe,Ni)_3P$, results in a release of diverse water-soluble phosphorus compounds which could serve as building blocks during prebiotic phosphorylation at the early stages of Earth evolution (Pasek et al. 2017; Kitadai and Maruyama 2018; Gibard et al. 2019). Other phosphides related to the Fe-Ni-P system (Table 1) were not considered for that role. However, our recent findings demonstrate that these minerals could be formed in a reducing environment of Archean era as well (Britvin et al. 2015). In that respect, unique catalytic and electrochemical properties of the synthetic counterpart of negevite, including its ability to photoinduced water splitting under soft conditions and hydrogenation activity (Gillot et al. 2005; Jiang et al. 2014), could provide new routes for further exploration of possible natural phosphorylation pathways . The discovery of negevite-bearing phosphide assemblages of the Mottled Zone undoubtedly imply the extremely reducing ("super-reducing") environment occurred during their crystallization. This enigma of the Hatrurim Formation is not yet resolved and requires gathering of further evidences.

Acknowledgments

This research was funded by Russian Science Foundation, grant 18-17-00079. We thank the referees, Evgeny Galuskin and Inna Lykova, for the helpful comments and discussion of the

manuscript. Associate Editor Fabrizio Nestola is thanked for handling of the review process. The authors thank X-ray Diffraction Centre, "Geomodel" Resource Centre and Nanophotonics Resoure Centre of St. Petersburg State University for providing instrumental and computational resources.

References cited

Barry, B.M., and Gillan, E.G. (2008) Low-temperature solvothermal synthesis of phosphorus-rich transition-metal phosphides. Chemistry of Materials, 20, 2618–2620.

Barry, B.M., and Gillan, E.G. (2009) A general and flexible synthesis of transition-metal polyphosphides via PCl_3 elimination. Chemistry of Materials, 21, 4454–4461.

Berzelius, J.J. (1832) Undersökning af en vid Bohumiliz I Böhmen funnen jernmassa. Kongelige Svenska Vetenskaps-Academiens Handlingar, 106–119.

Bindi, L., Cipriani, C., Pratesi, G., and Trosti-Ferroni, R. (2008) The role of isomorphous substitutions in natural selenides belonging to the pyrite group. Journal of Alloys and Compounds, 459, 553–556.

Britvin, S.N., Kolomensky, V.D., Boldyreva, M.M., Bogdanova, A.N., Kretser, Yu.L., Boldyreva, O.N., and Rudashevskii, N.S. (1999) Nickelphosphide, $(Ni,Fe)_3P$, the nickel analog of schreibersite. Zapiski Vsesoyuznogo Mineralogicheskogo Obshchestva, 128, 64–72 (in Russian).

Britvin, S.N., Rudashevsky, N.S., Krivovichev, S.V., Burns, P.C., and Polekhovsky, Y.S. (2002) Allabogdanite, $(Fe,Ni)_2P$, a new mineral from the Onello meteorite: The occurrence and crystal structure. American Mineralogist, 87, 1245–1249.

Britvin, S.N., Murashko, M.N., Vapnik, Ye., Polekhovsky, Yu.S., and Krivovichev, S.V. (2015) Earth's phosphides in Levant and insights into the source of Archaean prebiotc phosphorus. Scientific Reports, 5, 8355.

199 Britvin, S.N., Murashko, M.N., Vapnik, E., Polekhovsky, Yu.S., Krivovichev, S.V. (2017)
200 Barringerite Fe_2P from pyrometamorphic rocks of the Hatrurim Formation, Israel. Geology of
201 Ore Deposits, 59, 619–625.
202 Britvin, S.N., Murashko, M.N., Vapnik, Ye., Polekhovsky, Yu.S., Krivovichev, S.V., Vereshchagin,
203 O.S., Vlasenko, N.S., Shilovskikh, V.V., and Zaitsev, A.N. (2019a) Zuktamrurite, FeP_2, a new
204 mineral, the phosphide analogue of löllingite, $FeAs_2$. Physics and Chemistry of Minerals, 46,
205 361–369.
206 Britvin, S.N., Vapnik, Ye., Polekhovsky, Yu.S. and Krivovichev, S.V., Krzhizhanovkaya M.G.,
207 Gorelova L.A., Vereshchagin, O.S., Shilovskikh, V.V., and Zaitsev, A.N. (2019b)
208 Murashkoite, FeP, a new terrestrial phosphide from pyrometamorphic rocks of the Hatrurim
209 Formation, Southern Levant. Mineralogy and Petrology, 113, 237–248.
210 Bruker (2003) SAINT (ver. 7.60A). Bruker AXS Inc., Madison, Wisconsin, USA.
211 Buchwald, V.F. (1975) Handbook of iron meteorites. University of California Press, Berkeley, Los
212 Angeles, London.
213 Burg, A., Starinsky, A., Bartov, Y., and Kolodny, Ye. (1991) Geology of the Hatrurim Formation
214 ("Mottled Zone") in the Hatrurim basin. Israel Journal of Earth Sciences, 40, 107–124.
215 Buseck, P.R. (1969) Phosphide from meteorites: Barringerite, a new iron-nickel mineral. Science,
216 165, 169–171.
217 Dera, P., Lavina, B., Borkowski, L.A., Prakapenka, V.B., Sutton, S.R., Rivers, M.L., Downs, R.T.,
218 Boctor, N.Z., and Prewitt, C.T. (2008) High-pressure polymorphism of Fe_2P and its
219 implications for meteorites and Earth's core. Geophysical Research Letters, 35, L10301.
220 Dolomanov, O.V., Bourhis, L.J., Gildea, R.J., Howard, J.A., and Puschmann, H. (2009) OLEX2: a
221 complete structure solution, refinement and analysis program. Journal of Applied
222 Crystallography, 42, 339–341.

223 Donohue, P.C., Bither, T.A., and Young, H.S. (1968) High-pressure synthesis of pyrite-type nickel
224 diphosphide and nickel diarsenide. Inorganic Chemistry, 7, 998–1001.
225 Dowty, E. (2006). ATOMS for Windows. Shape Software, Kingsport, Tennessee, USA.
226 Galuskin, E.V., Kusz, J., Armbruster, T., Galuskina, I.O., Marzec, K., Vapnik, Ye., and Murashko,
227 M. (2013) Vorlanite, $(CaU^{6+})O_4$, from Jabel Harmun, Palestinian Autonomy, Israel. American
228 Mineralogist, 98, 1938–1942.
229 Galuskin, E.V., Galuskina, I.O., Kusz, J., Armbruster, T., Marzec, K., Dzierzanowski, P., and
230 Murashko, M. (2014) Vapnikite Ca_3UO_6 – a new double perovskite mineral from
231 pyrometamorphic larnite rocks of the Jebel Harmun, Palestine Autonomy, Israel.
232 Mineralogical Magazine, 78, 571–581.
233 Galuskina, I.O., Vapnik, Y., Lazic, B., Armbruster, T., Murashko, M., and Galuskin, E.V. (2014)
234 Harmunite $CaFe_2O_4$: a new mineral from the Jabel Harmun, West Bank, Palestinian
235 Autonomy, Israel. American Mineralogist, 99, 965–975.
236 Geller, Y.I., Burg, A., Halicz, L., and Kolodny, Y. (2012) System closure during the combustion
237 metamorphic ”Mottled Zone” event, Israel. Chemical Geology, 334, 25–36.
238 Gibard, C., Gorrell, I.B., Jimenez, E.I., Kee, T.P., Pasek, M.A., and Krishnamurthy, R. (2019)
239 Geochemical Sources and Availability of Amidophosphates on the Early Earth. Angewandte
240 Chemie, International Edition, 58, 8151–8155.
241 Gillot, F., Boyanov, S., Dupont, L., Doublet, M.-L., Morcrette, M., Monconduit, L., and Tarascon,
242 J.-M. (2005) Electrochemical reactivity and design of NiP_2 negative electrodes for secondary
243 Li-Ion Batteries. Chemistry of Materials, 17, 6327–6337.
244 Gross, S. (1977) The mineralogy of the Hatrurim Formation, Israel. Geological Survey of Israel
245 Bulletin, 70, 1–80.
246 Gu, T., Wu, X., Qin, S., and Dubrovinsky, L. (2011) In situ high-pressure study of FeP: Implications
247 for planetary cores. Physics of the Earth and Planetary Interiors, 184, 154–159.

248 Gu, T., Wu, X., Qin, S., Liu, J., Li, Y., and Zhang, Y. (2012) High-pressure and high-temperature in
249 situ X-ray diffraction study of FeP_2 up to 70 GPa. Chinese Physics Letters, 29, 026102.
250 Gu, T., Fei, Y., Wu, X., and Qin, S. (2014) High-pressure behavior of Fe_3P and the role of
251 phosphorus in planetary cores. Earth and Planetary Science Letters, 390, 296–303.
252 Hauff, P.L., Foord, E.E., Rosenblum, S., and Hakki, W. (1983) Hashemite, $Ba(Cr,S)O_4$, a new
253 mineral from Jordan. American Mineralogist, 68, 1223–1225.
254 Jiang, P., Liu, Q., and Sun, X. (2014) NiP_2 nanosheet arrays supported on carbon cloth: an efficient
255 3D hydrogen evolution cathode in both acidic and alkaline solutions. Nanoscale, 6, 13440–
256 13445.
257 Kerr, P.F. (1945) Cattierite and Vaesite: new Co-Ni minerals from the Belgian Congo. American
258 Mineralogist, 30, 483–497.
259 Khoury, H.N., Sokol, E.V., Kokh, S.N. Seryotkin, Yu.V., Kozmenko, O.A., Goryainov, S.V., and
260 Clark, I.D. (2016) Intermediate members of the lime-monteponite solid solutions ($Ca_{1-x}Cd_xO$,
261 x = 0.36–0.55): Discovery in natural occurrence. American Mineralogist, 101, 146–161.
262 Kitadai, N., and Maruyama, S. (2018) Origins of building blocks of life: A review. Geoscience
263 Frontiers, 9, 1117–1153.
264 Kolodny, Y., Burg, A., Geller, Y.I., Halicz, L., and Zakon, Y. (2014) Veins in the combusted
265 metamorphic rocks, Israel; Weathering or a retrograde event? Chemical Geology, 385, 140–
266 155.
267 Larsson, E. (1965) An X-ray investigation of the Ni-P system and the crystal structures of NiP and
268 NiP_2. Arkiv för Kemi, 23, 335–365.
269 Li, L., and Ghahreman, A. (2018) The synergistic effect of Cu^{2+}–Fe^{2+}–Fe^{3+} acidic system on the
270 oxidation kinetics of Ag-doped pyrite. The Journal of Physical Chemistry C, 122, 26897–
271 26909.

Möller, M.H., and Jeitschko, W. (1982) Darstellung, Eigenschaften und Kristallstruktur von Cu_2P_7 und Strukturverfeinerungen von CuP_2 und AgP_2. Zeitschrift für Anorganische und Allgemeine Chemie, 491, 225–236.

Murashko, M.N., Chukanov, N.V., Mukhanova, A.A., Vapnik, E., Britvin, S.N., Krivovichev, S.V., Polekhovsky, Yu.S., and Ivakin, Yu.D. (2010) Barioferrite $BaFe^{+3}_{12}O_{19}$ a new magnetoplumbite-group mineral from Hatrurim Formation, Israel. Geology of Ore Deposits, 53(7), 558–563.

Novikov, I., Vapnik, Ye., and Safonova, I. (2013) Mud volcano origin of the Mottled Zone, Southern Levant. Geoscience Frontiers, 4, 597–619.

Orishchin, S.V., Babizhet'sky, V.S., and Kuz'ma, Yu.B. (2000) Reinvestigation of the NiP_2 structure. Crystallography Reports, 45, 894–895.

Owens-Baird, B., Xu, J., Petrovykh, D.Y., Bondarchuk, O., Ziouani, Y., González-Ballesteros, N., Yox, P., Sapountzi, F.M., Niemantsverdriet, H., Kolen'ko, Yu.V., and Kovnir, K. (2019) NiP_2: a story of two divergent polymorphic multifunctional materials. Chemistry of Materials, 31, 3407–3418.

Papike, J.J., Ed. (1998) Planetary Materials, 36, 1052 p. Reviews in Mineralogy, Mineralogical Society of America, Chantilly, Virginia.

Pasek, M.A., Gull, M., and Herschy, B. (2017) Phosphorylation on the early earth. Chemical Geology, 475, 149–170.

Pauly, H. (1969) White cast iron with cohenite, schreibersite, and sulphides from Tertiary basalts on Disko, Greenland. Bulletin of the Geological Society of Denmark, 19, 8–26.

Pratesi, G., Bindi, L., and Moggi-Cecci, V. (2006) Icosahedral coordination of phosphorus in the crystal structure of melliniite, a new phosphide mineral from the Northwest Africa 1054 acapulcoite. American Mineralogist, 91, 451–454.

296 Scott, H.P., Huggins, S., Frank, M.R., Maglio, S.J., Martin, C.D., Meng, Y., Santillán, J., and
297 Williams, Q. (2007) Equation of state and high-pressure stability of Fe_3P-schreibersite:
298 Implications for phosphorus storage in planetary cores. Geophysical Research Letters, 34,
299 L06302.
300 Sharygin, V.V., Lazic, B., Armbruster, T.M., Murashko, M.N., Wirth, R., Galuskina, I., Galuskin,
301 E.V., Vapnik, Ye., Britvin, N., and Logvinova, A.M. (2013) Shulamitite $Ca_3TiFe^{3+}AlO_8$ – a
302 new perovskite-related mineral from Hatrurim Basin, Israel. European Journal of Mineralogy,
303 25, 97–111.
304 Sheldrick, G.M. (2015) Crystal structure refinement with *SHELXL*. Acta Crystallographica, C71, 3–
305 8.
306 Sokol, E.V., Maksimova, N.V., Nigmatulina, E.N., Sharygin, V.V., and Kalugin, V.M. (2005)
307 Combustion Metamorphism, 284 p. Publishing House of the Siberian Branch of the Russian
308 Academy of Science, Novosibirsk (in Russian).
309 Sokol, E.V., Gaskova, O.L., Kokh, S.N., Kozmenko, O.A., Seryotkin, Y.V., Vapnik, Y., Murashko,
310 M.N. (2011) Chromatite and its Cr^{3+}- and Cr^{6+}-bearing precursor minerals from the Nabi Musa
311 Mottled Zone complex, Judean Desert. American Mineralogist, 96, 659–674.
312 Vapnik, Ye., Sharygin, V.V., Sokol, E.V., and Shagam, R. (2007) Paralavas in a combustion
313 metamorphic complex: Hatrurim Basin, Israel. The Geological Society of America, Reviews in
314 Engineering Geology, 18, 133–153.
315 Vinogradova, R.A., Rudashevskii, N.S., Bud'ko, I.A., Bochek, L.I., Kaspar, P., and Padera, K.
316 (1976): Krutovite – a new cubic nickel diarsenide. Zapiski Vsesoyuznogo Mineralogicheskogo
317 Obshchestva, 105, 59–71 (in Russian).
318 Weber, D., and Bischoff, A. (1994) Grossite ($CaAl_4O_7$) – a rare phase in terrestrial and
319 extraterrestrial rocks. European Journal of Mineralogy, 6, 591–594.
320

List of figure captions

Figure 1. Negevite in phosphide assemblages of the Halamish wadi, Hatrurim Basin, Southern Negev Desert, Israel. (A) Photomicrograph in reflected light. (B) The same area, SEM BSE image. (C) Element distribution map for phosphorus. (D) Element distribution map for iron and nickel. Abbreviations: Ng, negevite (NiP_2); Zk, zuktamrurite (FeP_2); Tj, transjordanite (Ni_2P). (Color online.)

Figure 2. Fractured grain of Ag-bearing negevite among secondary Ca-Fe-silicates in altered pyroxene-anorthite paralava. Note grains of Ag-free transjordanite and zuktamrurite associated with negevite. Daba-Siwaqa complex, Transjordan plateau, Jordan. SEM BSE image. Abbreviations: Ng, negevite (NiP_2); Zk, zuktamrurite (FeP_2); Tj, transjordanite (Ni_2P).

Figure 3. Crystal structure of negevite (pyrite structure type). (A) General view: corner-sharing [NiP_6] octahedra (green) linked by P–P "dumbbell" bonds (yellow) characteristic of the pyrite structure. (B) Skeletal view of [NiP_6] octahedron connected to [$P(Ni_3P)$] tetrahedra. (C) Slice of substructure framework composed of corner-sharing [NiP_6] octahedra. (D) Slice composed of [$P(Ni_3P)$] tetrahedra. Legend: green, Ni [4*a*; 0, 0, 0]; yellow, P [8*c*; 0.3844(1), *x*, *x*]. (Color online.)

Tables

Table 1. Natural phosphides related to the Fe-Ni-P system

Mineral	End member	Structure type	Occurrence [a]	Reference
Schreibersite	Fe_3P	Fe_3P ($I\bar{4}$)	M T	Berzelius (1832)
Barringerite	Fe_2P	Fe_2P ($P\bar{6}2m$)	M T	Buseck (1969); Britvin et al. (2017)
Allabogdanite	Fe_2P	Co_2Si (*Pnma*)	M	Britvin et al. (2002)
Murashkoite	FeP	MnP (*Pnma*)	T	Britvin et al. (2019b)
Zuktamrurite	FeP_2	Marcasite (*Pnnm*)	T	Britvin et al. (2019a)
Melliniite	$(Ni,Fe)_4P$ [b]	Au_4Al ($P2_13$)	M	Pratesi et al. (2006)
Nickelphosphide	Ni_3P	Fe_3P ($I\bar{4}$)	M	Britvin et al. (1999)
Nazarovite	$Ni_{12}P_5$	$Ni_{12}P_5$ ($I4/m$)	M T	Britvin et al. (2019c) [c]
Transjordanite	Ni_2P	Fe_2P ($P\bar{6}2m$)	T	Britvin et al. (2015)
Orishchinite	Ni_2P	Co_2Si (*Pnma*)	T	Britvin et al. (2019d) [c]
Halamishite	Ni_5P_4	Ni_5P_4 ($P6_3mc$)	T	Britvin et al. (2015)
Negevite	NiP_2	Pyrite ($Pa\bar{3}$)	T	This work

[a] Occurrence: M – meteoritic; T – terrestrial (the Hatrurim Formation). [b] End-member is not known.
[c] Approved by the Commission on New Minerals, Nomenclature and Classification of International Mineralogical Association, IMA 2019-013 (nazarovite) and 2019-039 (orishchinite).

This is a preprint, the final version is subject to change, of the American Mineralogist (MSA)
Cite as Authors (Year) Title. American Mineralogist, in press.
DOI: https://doi.org/10.2138/am-2020-7192

Table 2. Chemical composition of negevite and associated phosphides

Mineral [a]	Ng	Ng	Ng	Tj	Zk	Ng	Zk	Tj
Locality [b]	HB	HB	HB	HB	HB	DS	DS	DS
Notes	Holotype		Fig. 1	Fig. 1	Fig. 1	Fig. 2	Fig. 2	Fig. 2
				Wt%				
Ni	42.57	38.25	37.77	71.95	8.83	38.79	15.66	74.80
Co	3.40	2.92	3.44	0.30	1.24	3.40	0.37	0.15
Fe	2.87	6.15	6.41	6.26	36.74	5.12	30.87	3.30
Ag	-	-	-	-	-	1.01	-	-
P	42.93	40.05	40.07	21.14	52.25	39.51	51.43	21.09
S	8.33	12.12	12.78	0.00	1.51	10.82	0.00	0.00
Se	-	-	0.24	-	-	-	-	-
Total	100.10	99.49	100.71	99.65	100.57	98.65	98.33	99.34
				Formula amounts (3 *apfu*)				
Ni	0.88	0.79	0.77	1.82	0.18	0.82	0.32	1.90
Co	0.07	0.06	0.07	0.01	0.02	0.07	0.01	0.00
Fe	0.06	0.13	0.14	0.17	0.77	0.11	0.67	0.09
Ag						0.01		
Σ	1.01	0.98	0.98	2.00	0.97	1.01	1.00	1.99
P	1.68	1.56	1.55	1.01	1.97	1.57	2.00	1.01
S	0.31	0.46	0.48		0.06	0.42		
Se			0.004					
Σ	1.99	2.02	2.03	1.01	2.03	1.99	2.00	1.01

[a]Abbreviations: Ng, negevite; Tj, transjordanite; Zk, zuktamrurite. [b]Localities: HB, Hatrurim Basin, Israel; DS, Daba-Siwaqa complex, Jordan. [c]The bar "-" denotes below detection limit (<0.05 wt%).

This is a preprint, the final version is subject to change, of the American Mineralogist (MSA)
Cite as Authors (Year) Title. American Mineralogist, in press.
DOI: https://doi.org/10.2138/am-2020-7192

Table 3. Unit cell parameters of negevite and related minerals and compounds

Mineral	Negevite	Synthetic	Vaesite	Krutovite	Penroseite
Ideal formula	NiP_2	NiP_2	NiS_2	$NiAs_2$	$NiSe_2$
a (Å)	5.4816	5.4475	5.6679	5.7634	5.988
Reference [a]	[1]	[2]	[3]	[4]	[5]

[a] [1] This work; [2] Owens-Baird et al. (2019); [3] Kerr (1945); [4] Donohue et al. (1968); Vinogradova et al. (1976); [5] Bindi et al. (2008).

This is a preprint, the final version is subject to change, of the American Mineralogist (MSA)
Cite as Authors (Year) Title. American Mineralogist, in press.
DOI: https://doi.org/10.2138/am-2020-7192

Figures

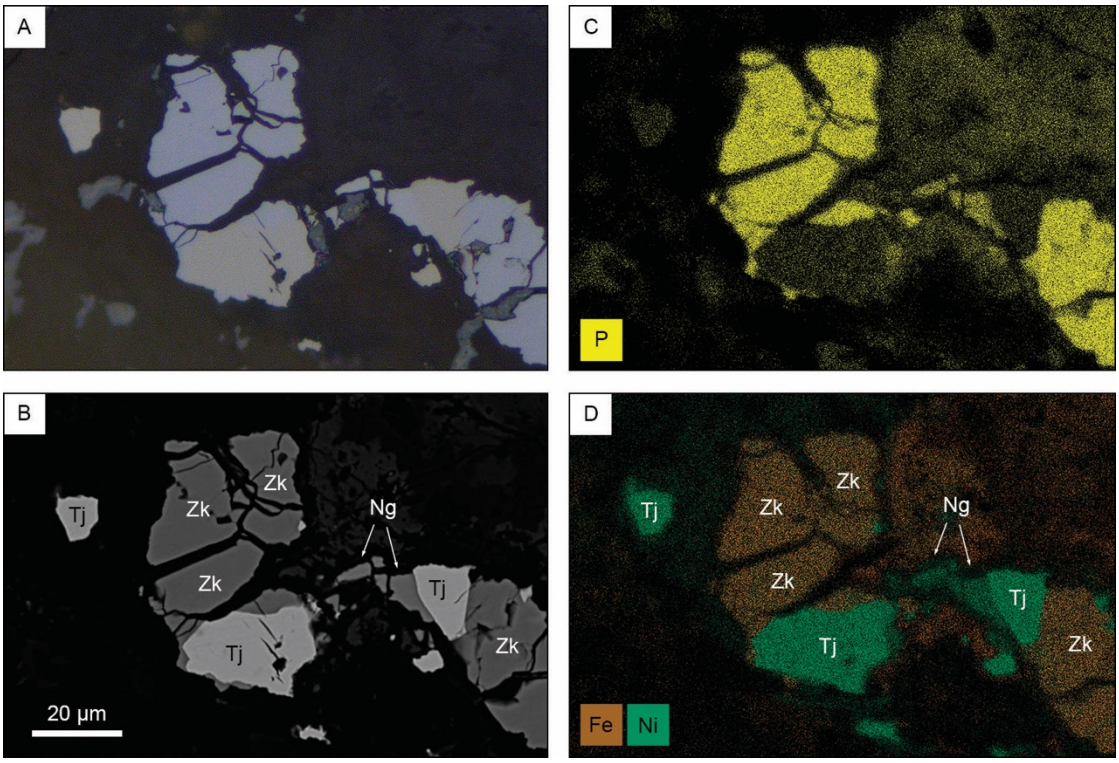

Figure 1

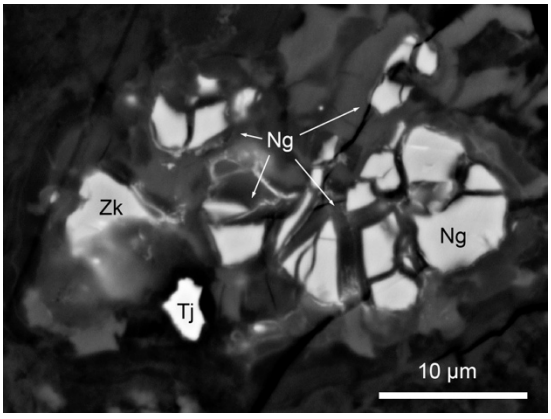

Figure 2

This is a preprint, the final version is subject to change, of the American Mineralogist (MSA)
Cite as Authors (Year) Title. American Mineralogist, in press.
DOI: https://doi.org/10.2138/am-2020-7192

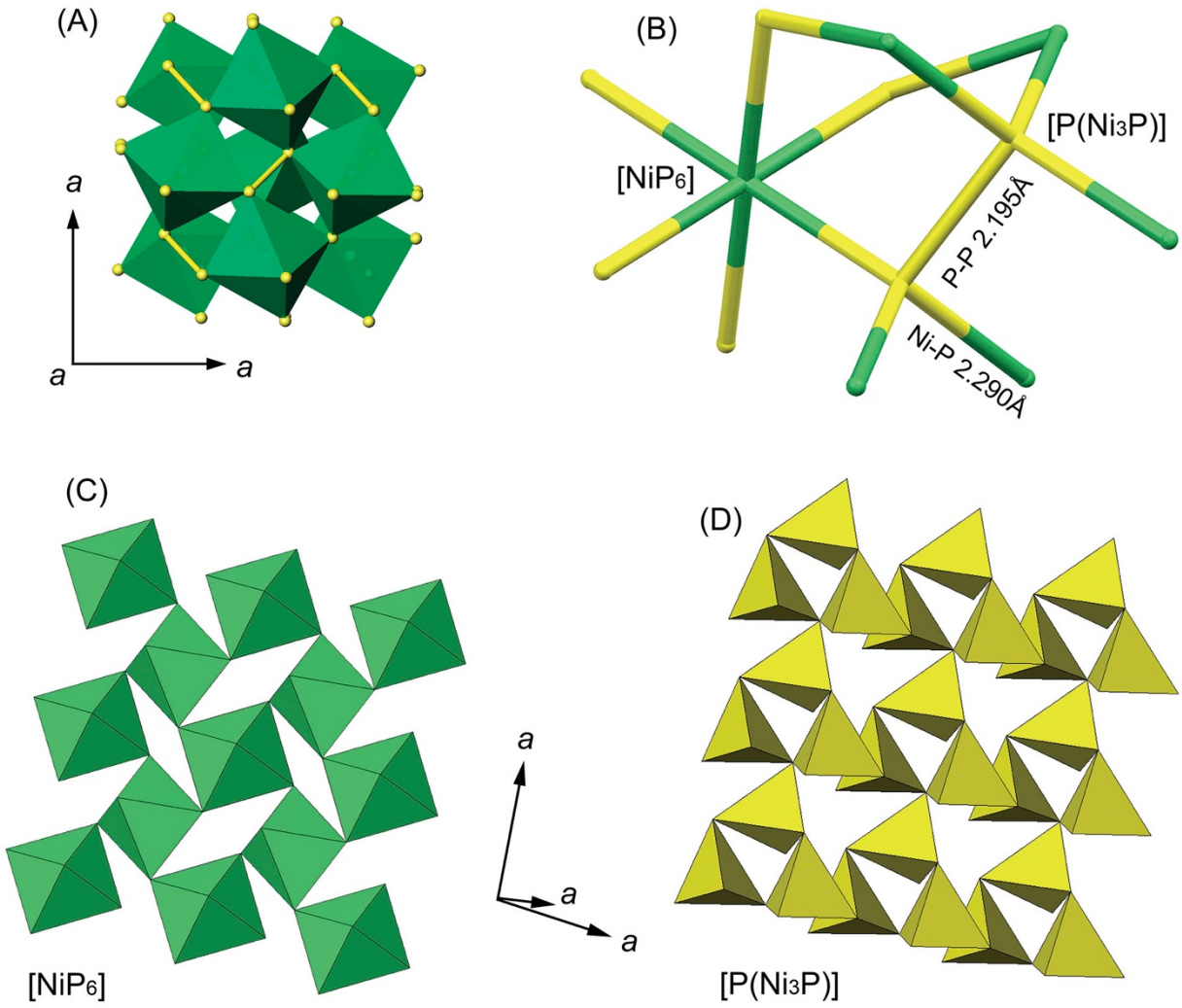

Figure 3